In Situ Measurement of Electrode Surface Change by Photoacoustic Spectroscopy

Hideki MASUDA, Akira FUJISHIMA,* and Kenichi HONDA

Department of Synthetic Chemistry, Faculty of Engineering, The University of Tokyo, Hongo, Bunkyo-ku, Tokyo 113

(Received December 25, 1979)

Photoacoustic spectroscopy (PAS) was used for the study of electrode-electrolyte interfaces *in situ*. The design of the PAS cell and the experimental procedure are given. The change in absorption at the interface during electrochemical reaction at Au electrodes, as measured by PAS technique, is described.

In resent years, there has been much interest in photoacoustic spectroscopy (PAS)[1-4] as a new tool for the investigation of the surface condition of various materials. One of the advantages of PAS is that absorption spectra can be obtained even for solid samples that are difficult to measure by conventional spectroscopic techniques on account of light scattering problems. We have noted this characteristics of PAS from the viewpoint of spectro-electrochemistry, and attemped to apply PAS to studies of the electrode surface *in situ*. Generally, spectro-electrochemical behavior is measured by using an electrode that is optically transparent,[5,6] internally reflective,[7,8] or specularly reflective,[9,10] by ellipsometric techniques,[11,12] and so on, for the purpose of characterizing the electrode-solution interfaces, or measuring the kinetic behavior of electrode reaction. It is expected that PAS will be more advantageous than conventional spectroscopic techniques in observing the electrode-solution interfaces, because preparation of a sample electrode is not difficult, that is, the surface does not need to be highly polished. Some work has been reported on the application of PAS to electrochemical studies,[13,14] but PAS was used in these cases to measure the absorption spectra of the electrode surface in the air after removal from the electrolysis cell. Here, we have applied PAS to study the surface behavior of metal electrode *in situ*.

In a conventional PAS cell, a sample is placed inside a closed chamber containing a suitable gas, and is illuminated through a window. For *in situ* investigation of an electrode surface that is in contact with the solution, such a cell can not be used in the usual way. Another technique for measuring electrode surfaces by PAS used a piezo electric pressure transducer,[15,16] but this method seems unsuitable for a solid-liquid system, especially an electrochemical one in which gas evolution may occur by electrolysis because the presence of bubbles in the solution would adversely affect the acoustic signal.

Therefore we constructed another type of cell, in which the sample was mounted outside the gas chamber. Heat on the surface of the sample resulting from radiationless transition due to irradiation with light is transported to the rear of the sample, causing the sealed gas to expand. Until now this technique has been scarcely used, because it has been thought that in the case of relatively thick samples the photoacoustic signal in this type of cell is liable to decrease during the conduction of heat from the active surface to the rear. As exceptional examples, Kanstad *et al.* measured the middle infrared region PAS spectra of specimens kept on a thin Al plate called open membrane spectrophone,[17] and Adams *et al.* applied this type of cell to determine the thermal diffusibility of thin polymer films.[18] Since even in these cells, the photoacoustic signals did not seem to decrease significantly, this technique can be put to practical use. The present work is concerned with the photoacoustic signal change in electrode-solution interfaces in the course of the electrode reaction, oxidation of an Au electrode or electrochemical deposition of other metals on the Au electrode.

Experimental

Figure 1 shows detail of the PAS cell employed in this study. The PAS cell was constructed from acrylic resin and used for spectroscopic measurement in electrolytic solutions. This PAS cell was 3.0 cm in width and 7.0 cm in height, and its internal volume was approximately 0.4 cm^3. An electret condenser microphone (Sony Model ECM-150) was employed in this cell as a pressure transducer. The working electrode was a flat gold plate 0.1 mm thick and 7.0 mm in diameter, which was polished to a bright surface with 3 μm alumina powder and then mounted on one side of the PAS cell by a silicone O-ring to ensure an air-tight seal. In this work, a PAS cell of the ordinary type was also used as a control for the results obtained using the cell shown in Fig. 1.

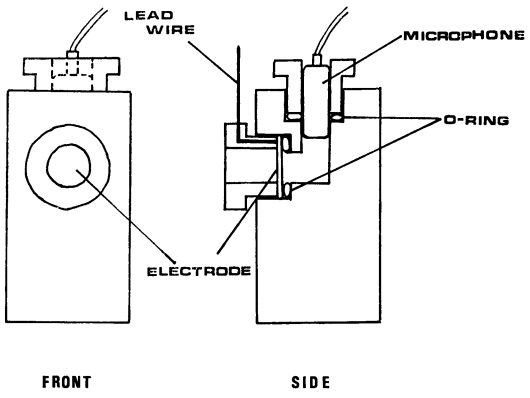

Fig. 1. PAS cell and sample arrangement.

Figure 2 shows the experimental set up. The light source was either a 500 W Xe lamp (Ushio Electric) or 3 W Ar ion laser (Spectra Physics Model 164). In measuring the photoacoustic spectrum using the Xe lamp, the radiation was focused on the electrode surface using a convex lens through a series of 10 nm bandwidth interference filters (Koshin Kogaku) and the light intensities of each wavelength were

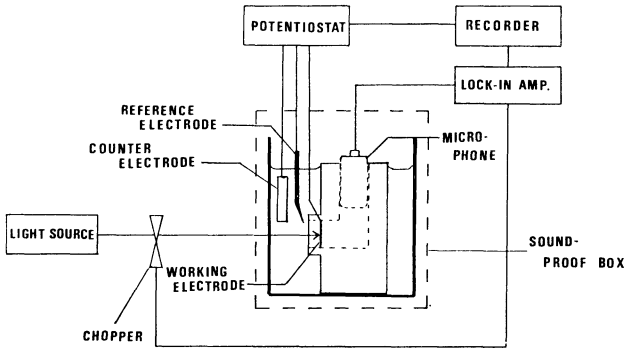

Fig. 2. Experimental set up for PAS–electrode system.

normalized by comparison with spectrum of carbon measured under identical conditions. The diameter of the laser beam was approximately 1.5 mm. The light beam was chopped mechanically by light chopper and the photoacoustic signal detected by the microphone was fed to a lock-in amplifier (Brookdeal Model 9501, or Nihon Bunko Model LA-120). The measurement was carried out using a chopping frequency of 125 Hz by considering both of the light power per pulse and the frequency characteristics of the microphone employed in this work. Electrolysis was carried out in a pyrex cell which had an optically flat window. This cell was held in a lead box to reduce external acoustic noises. A potentiostat (Nikko Keisoku Model NPGS-301) with a potential programmer (Nikko Keisoku Model NPS-2) was used to obtain current-potential curves. A saturated calomel electrode (SCE) was used as a reference electrode and the counter electrode was of platinum. A coulometer (Kowa Electronics Model DCM-150) was used to determine the total charge. The influence upon the photoacoustic signal of temperature changes resulting from electrode reactions, which is known as the electrochemical peltier effect,[19] was considered to be negligible because only the AC component of temperature change was detected by the lock-in amplifier. Current-potential, photoacoustic signal-potential and photoacoustic signal-charge curves were recorded on a X-Y-Y′ recorder (Riken Denshi Model D-72 or Yokokawa Model 3078).

Results and Discussion

Open Membrane Type Photoacoustic Cell. Before a measurement with the PAS cell shown in Fig. 1, we checked whether this cell could work well or not. Then, the photoacoustic signal at the open membrane type cell (Fig. 3A, the same type as that in Fig. 1) was compared with that of the conventional type cell

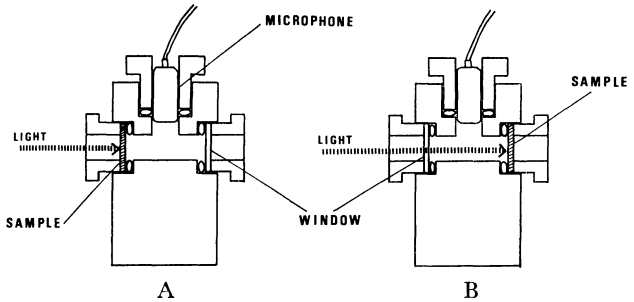

Fig. 3. Schematic diagram for measurement of signal magnitude. A) Open membrane type, B) conventional type.

Table 1. Comparison of the magnitudes of signals of PAS
(Irradiation by Ar ion laser, 0.5 W, 514.5 nm, 125 Hz)

	(A) Open membrane type	(B) Conventional type
Carbon (0.5 mm)	17 (μV)	44 (μV)
Au plate (0.1 mm)	19 (μV)	35 (μV)
Au plate (0.05 mm)	42 (μV)	35 (μV)

(Fig. 3B), where ways of irradiation to the sample were different. Table 1 shows the magnitude of the photoacoustic signal for a glassy carbon pellet and Au plates with the both cells. The signals were affected by the condition of the surfaces, especially in that of the Au plates. However, for the samples tested, the magnitude of the photoacoustic signals of the open membrane type cell was not significantly smaller than those of the conventional type cell. Further, for the thin Au plate (0.05 mm) the signal was observed to be larger than that of the conventional type cell, perhaps because in the latter illuminating intensity decreased on account of reflection at the glass window.

Even when the open membrane cell was immersed in the solution so that the sample surface was in contact with the solution, the photoacoustic signals did not decrease greatly. The signal ratio S(solution)/S(air) was approximately 0.9 in the case of the Au plate. These results show that the open membrane type PAS cell is well suited for practical use. Therefore, results shown below were obtained by use of the PAS cell shown in Fig. 1 (*i.e.* the open membrane type PAS cell).

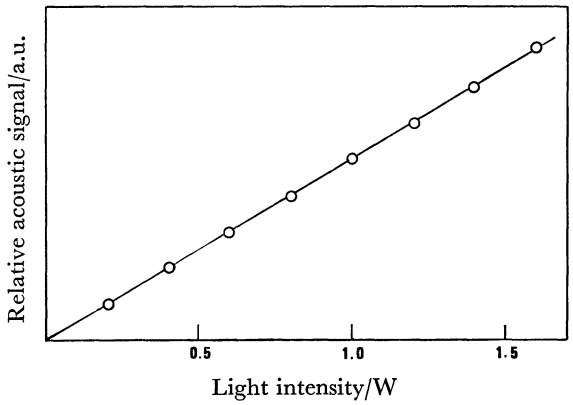

Fig. 4. Relationship between signal magnitude and incident light intensity for Au plate.

Figure 4 shows the relationship between the magnitude of the acoustic signal and the incident light intensity for the Au plate, where irradiation was carried out using the Ar ion laser (514.5 nm). The plot of the PAS signal against light intensity is relatively linear, and we consider that the photoacoustic signal does not appear to reach saturation even in high intensity region observed in this study.

Measurement of the Electrochemical Deposition of Cu on Au Electrode. Figure 5 shows the photoacoustic spectra

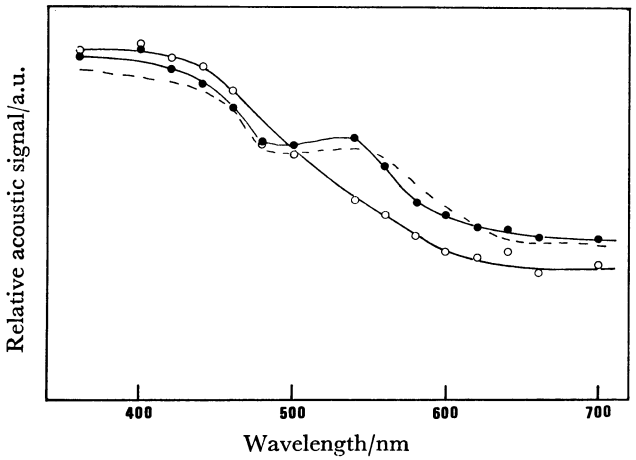

Fig. 5. Photoacoustic spectra of Au electrode; before (-○-), after (-●-) electrotysis in 5×10^{-3} M Cu^{2+} and of Cu plate (------).

of the Au electrode before and after electrolysis at −0.2 V *vs.* SCE in 1 M $HClO_4$ (1 M=1 mol/dm^3) containing 5×10^{-3} M Cu^{2+}, along with that of a 0.05 mm thick Cu plate, which was measured separately. Since the spectrum after electrolysis agreed with that of the Cu plate, it indicates that the Au electrode surface was covered with a Cu layer.

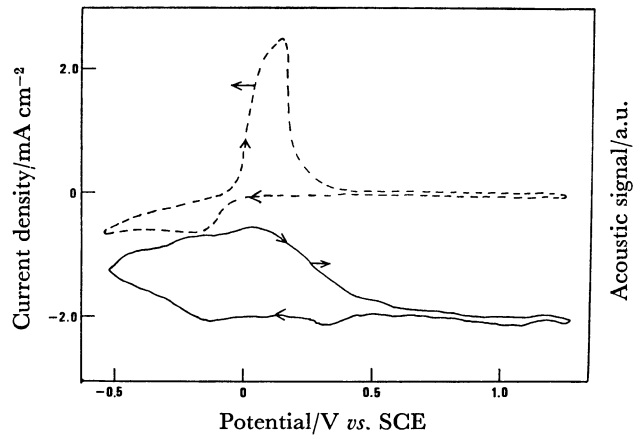

Fig. 6. Photoacoustic signal *vs.* potential (——) and current *vs.* potential (------) curves of Au electrode in the presence of Cu^{2+} ion.
5×10^{-3} M Cu^{2+}, 1 M $HClO_4$, potential sweep rate 40 s/V, λ=514.5 nm.

Figure 6 is a plot of the photoacoustic signal *versus* potential and current *versus* potential curves in the same electrolyte solution as in Fig. 5. The result in Fig. 5 shows that the light absorption of Cu is larger than that of Au when irradiated by a 514.5 nm Ar ion laser. The reduction current around −0.1 V in the cathodic sweep was due to the electrochemical deposition of Cu, and at almost the same potential it was observed that the photoacoustic signal began to increase. On the other hand, the anodic current peak at 0.20 V was attributed to the dissolution of the Cu layer. At that time the photoacoustic signal began to decrease

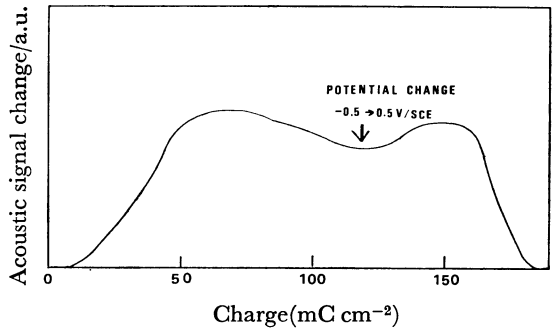

Fig. 7. Relative change in photoacoustic signal *vs.* charge for electrochemical deposition of Cu.
5×10^{-3} M Cu^{2+}, 1 M $HClO_4$, potential −0.5 V and +0.5 V *vs.* SCE. λ=514.5 nm.

and then returned to the value for the bare Au surface.

Figure 7 shows the change in the photoacoustic signal relative to the electric charge associated with the electrochemical deposition of Cu on the Au surface at −0.5 V. The photoacoustic signal increased in proportion to the charge and then became the constant value at about 50 mC/cm^2. At this charge, the thickness of the deposited copper layer was estimated to be 20 nm, assuming that the layer was uniform. The linear relationship between the photoacoustic signal and the charge can be interpreted on the basis of the McIntyre-Aspnes approximation,[20] in which the change in reflectivity is proportional to the thickness of thin film formed. In the flat region the photoacoustic signal would seem to be the result of absorption at the Cu layer alone. As shown in Fig. 7, the photoacoustic signal decreased a little in the region where the deposited layer became thicker. The reason for this is uncertain, but one can assume that one of the reasons is an increase in the surface heat radiation as the rough copper layer is formed. In anodic reaction, the photoacoustic signal decreased on a reverse path until it reached the value for the bare Au surface.

In *in situ* measurements such as those in Figures 6 and 7, the time constant of the phase sensitive detection is one of the significant factors. When the time constant is large compared with the reaction rate, a time lag is liable to be caused in the photoacoustic signal change.

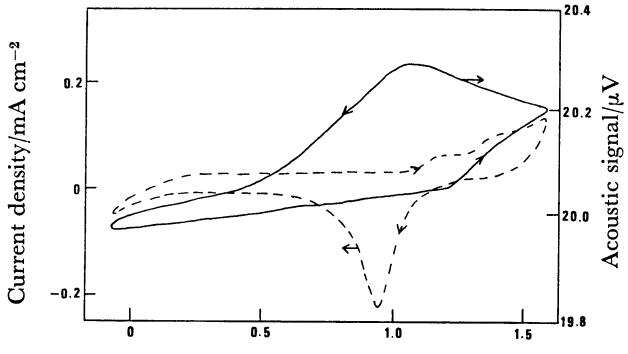

Fig. 8. Photoacoustic signal *vs.* potential (——) and current *vs.* potential (------) curves of Au electrode.
1 M $HClO_4$, potential sweep rate 40 s/V, λ=514.5 nm.

In this work, the photoacoustic signal was measured at a time constant of 1—3 s.

Measurement of Formation of an Oxide Layer at Au. Figure 8 shows the curve for the photoacoustic signal *versus* applied potential together with a current *versus* potential curve in 1 M $HClO_4$ solution on an Au electrode where photoacoustic signal was measured at a wavelength of 514.5 nm from the Ar ion laser with light intensity of 0.8 W. It has been widely reported that oxide layers are formed on the Au electrode with anodic polarization in an acid solution.[21-24] The anodic current at 1.2 V in the anodic sweep was attributed to the formation of the oxide layer on the Au electrode. As shown in Fig. 8 the increase in the photoacoustic signal began at almost the same potential as increase of the anodic current. The increase in the photoacoustic signal was mainly due to the increase in absorption resulting from formation of the oxide layer on the Au electrode, because the absorption coefficient of the oxide is greater than that of Au irradiated at 514.5 nm. On the other hand, in the cathodic sweep, a current peak was observed around 0.9 V due to the reduction of the oxide layer and at that time the photoacoustic signal decreased gradually depending on the amount of cathodic electricity. When the cathodic current decreased to the original value around 0.65 V, the photoacoustic signal also showed the same value as that on the bare Au surface.

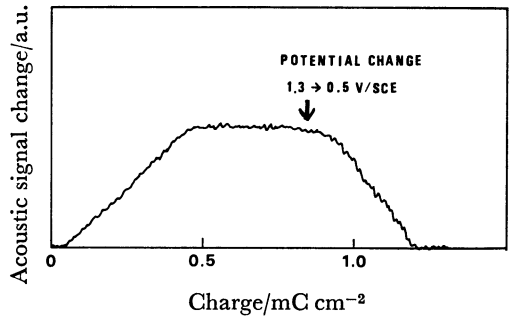

Fig. 9. Relative change in photoacoustic signal *vs.* charge for the formation of gold oxide.
1 M $HClO_4$, potential +1.3 V and 0.5 V *vs.* SCE. λ=514.5 nm.

Figure 9 shows the relationship between the change in the relative photoacoustic signal and the charge flowing. Figure 9 also showed the change in the photoacoustic signal, stepping the applied potential from 1.3 V to 0.5 V, at which potential the oxide is reduced. In Fig. 9 the photoacoustic signal increased linearly with the quantity of electricity for the oxidation process, and then reached a constant at about 0.5 C/cm^2, where the thickness of the oxide layer was estimated to be 0.5 nm, assuming the composition of the oxide layer to be Au_2O_3 with a bulk density of 6 g/cm^3.[24] In the rising region in Fig. 9, the acoustic signal seems to increase in proportion to the degree of surface coverage of the oxide layer. When the oxide layer was reduced by changing the applied potential from 1.3 V to 0.5 V, the photoacoustic signal decreased to the value at the bare Au surface.

Conclusion. The instrumentation used is simple and unsophisticated, but this technique was found to be useful for the study of electrode-solution interfaces *in situ*.[25] This PAS technique may be applicable for kinetic studies concerning electrode reactions, as well as for qualitative analysis by spectroscopic measurement. Sensitivity was fairly high, *e.g.*, in the order of monolayer change when using laser irradiation, and could be further improved by modification of the PAS cell, *e.g.*, smaller internal cell volume. Since PAS is influenced by external acoustic noises, exhaustive counterplan against the acoustic noise would be also required. In addition, by employing a double-beam PAS system, the signal to noise ratio could be expected to improve.

This technique is considered to be applicable to any type of samples (*e.g.* rough or porous surfaces) which are difficult to examine by conventional techniques. Since the metal electrodes employed in this work had flat, highly reflective surface, photoacoustic signals were relatively small. Semiconductors, however, have more definitive characteristics especially concerning their light effect, so this technique would be more useful for their electrode systems.

References

1) W. R. Harshbarger and M. B. Robin, *Acc. Chem. Res.*, **6**, 329 (1973).
2) A. Rosencwaig, *Anal. Chem.*, **47**, 592A (1975).
3) M. J. Adams, A. A. King, and G. F. Kirkbright, *Analyst*, **101**, 73 (1976).
4) R. C. Gray, V. A. Fishman, and A. J. Bard, *Anal. Chem.*, **49**, 697 (1977).
5) W. Benken and T. Kuwana, *Anal. Chem.*, **42**, 1114 (1970).
6) W. R. Heineman and T. Kuwana, *Anal. Chem.*, **43**, 1075 (1971).
7) W. N. Hansen and J. A. Horton, *Anal. Chem.*, **36**, 783 (1964).
8) W. N. Hansen, T. Kuwana, and R. A. Osteryoung, *Anal. Chem.*, **38**, 1810 (1966).
9) D. F. A. Koch, *Nature*, **202**, 387 (1964).
10) J. D. E. McIntyre, "Advance in Electrochemistry and Electrochemical Engineering," J. Wiley and Sons, New York (1973), Vol. 9, pp. 61—166.
11) J. Kruger, *J. Electrochem. Soc.*, **110**, 654 (1963).
12) W. Paik, M. A. Genshaw, and J. O'M. Bockris, *J. Phys. Chem.*, **74**, 4266 (1970).
13) P. Nordal and S. O. Kanstad, *Opt. Commun.*, **24**, 95 (1978).
14) M. Fujihira, T. Osa, D. Hursh, and T. Kuwana, *J. Electroanal. Chem.*, **88**, 285 (1978).
15) W. Lahmann, H. J. Ludewig, and H. Welling, *Anal. Chem.*, **49**, 549 (1977).
16) S. Oda, T. Sawada, and H. Kamada, *Anal. Chem.*, **50**, 865 (1978).
17) S. O. Kanstad and P. Nordal, *Opt. Commun.*, **26**, 367 (1978).
18) M. J. Adams and G. F. Kirkbright, *Analyst*, **102**, 281 (1977).
19) R. Tamamushi, *J. Electroanal. Chem.*, **45**, 500 (1973); **65**, 263 (1975).
20) J. D. E. McIntyre and D. E. Aspnes, *Surf. Sci.*, **24**, 417 (1971).

21) W. E. Reid and J. Kruger, *Nature*, **203**, 402 (1964).
22) R. S. Sirohi and M. A. Genshaw, *J. Electrochem. Soc.*, **116**, 910 (1969).
23) T. Takamura, K. Takamura, W. Nippe, and E. Yeager, *J. Electrochem. Soc.*, **117**, 626 (1970).
24) D. M. Kolb and J. D. E. McIntyre, *Surf. Sci.*, **28**, 321 (1971).
25) A. Fujishima, H. Masuda, and K. Honda, *Chem. Lett.*, **1979**, 1063.